Materials Science-Poland, *Vol. 28*, *No. 3*, *2010*

A study on the synthesis, characterization and photocatalytic activity of TiO_2 derived nanostructures

B. ZIELIŃSKA*, E. BOROWIAK-PALEN, R. J. KALENCZUK

Institute of Chemical and Environment Engineering, West Pomeranian University of Technology, Szczecin, Pułaskiego 10, 70-322, Szczecin, Poland

Syntheses of TiO_2 derived nanostructures have been conducted at 210 °C by hydrothermal reaction of commercial TiO_2-P25 (Degussa, Germany) in 10 M NaOH aqueous solution. High purity of the as-produced material was confirmed by scanning and transmission electron microscope analyses. The crystallographic structure, as well as the optical and vibronic properties of this material were examined by X-ray diffraction, diffuse reflectance (DR) UV-Vis, resonance Raman spectroscopic methods, respectively. Detailed analysis of the phase composition revealed that the rod-like structures are made up of sodium tetratitanate ($Na_2Ti_4O_9$). It was also observed that acid treatment of the material (hydrothermal reaction) led to a decrease in the diameters of the nanorods. Finally, the photocatalytic activity of the investigated nanostructures was examined, by observing the reaction photocatalytic decolourisation of two organic dyes (Reactive Red 198 and Reactive Black 5) under UV-light irradiation.

Keywords: *nanostructures; oxides; chemical synthesis;*

1. Introduction

Over recent decades, syntheses and characterization of one-dimensional (1D) nanostructures such as nanotubes, nanorods and nanofibres have received significant attention, due to their unusual physical and chemical properties and wide range of potential applications [1–3]. The most outstanding example of a 1D nanostructure is the carbon nanotube [4–6]. However, other one dimensional nanomaterials including metals, oxides or nitrides have also been intensively studied [3, 7–10]. It was noticed that 1D oxidic nanostructures can offer many remarkable advantages which lead to new technological applications, particularly in nanoelectronics and nanophotonics [11].

*Corresponding author, e-mail: bzielinska@zut.edu.pl

Among 1D oxidic nanomaterials, TiO_2 is one of the most interesting. Recently, a large number of synthesis experiments of TiO_2 derived nanotubes, nanorods and nanowires have been reported. Various methods for preparation of those materials have been tested such as combining sol-gel processing with electrophoretic deposition, spin-on processes, anodic oxidative hydrolysis, sonochemical synthesis and pyrolysis routes [12–14]. Nevertheless, one of the most promising and simple methods for synthesizing TiO_2 derived nanostructures is hydrothermal treatment of titania powders of various crystallographic structures (rutile, anatase, and brookite) in a strongly alkaline aqueous solution of NaOH. These methods do not require any templates and the obtained nanostructures have smaller diameter of ca. 10 nm, and high crystallinity [15, 16]. At first, TiO_2-derived nanotubes with a diameter of about 8 nm were obtained by hydrothermal treatment of rutile powders in 10 M NaOH solution at 110 °C [15].

In spite of many studies on the structures and proposed formation mechanisms of the products of the alkaline hydrothermal treatment, it is still a controversial and constantly debated topic among the research community. At first, it was believed that the products of the hydrothermal synthesis with NaOH are nanotubes and nanorods of anatase [1–15]. Afterwards, it was reported that nanotubes of $H_2Ti_3O_7$ are formed and that NaOH acts only as a catalyst [17]. Later, Yang et al. [18] found that the produced nanotubes are $Na_2Ti_2O_4(OH)_2$ but not TiO_2. Next, Sun et al. [19] argued that TiO_2 derived nanotubes are titanates of $Na_xH_{2-x}Ti_3O_7$ type. Additionally, it was also reported that thermal behaviour of TiO_2 derived nanotubes and nanorods are different. Such nanotubes are usually unstable at higher temperatures (above 500 °C) and break down into anatase particles, whereas nanorods converted to the metastable TiO_2 B phase keep their morphology [20, 21].

In the present study, TiO_2-derived nanostructures were produced by a hydrothermal reaction using 10M NaOH aqueous solution and TiO_2-P25 (Degussa, Germany) as precursors. The reaction was carried out at 210 °C. Crystallographic composition, optical and vibronic properties of the product were also investigated. Furthermore, the effect of acid treatment on the morphology of the material was investigated. Finally, the photocatalytic activity of the investigated nanostructures was examined, by observing the photocatalytic decolourisation of two organic dyes (Reactive Red 198 and Reactive Black 5) under UV-light irradiation.

2. Experimental

Materials. Commercial titanium dioxide with a crystalline structure of ca. 20% rutile and ca. 80% anatase and primary particle size of ca. 25 nm (TiO_2–P25, Degussa, Germany) and sodium hydroxide (NaOH, Sigma-Aldrich) were used as the starting materials for the synthesis of the TiO_2-derived nanostructures.

Reactive Red 198 (RR198) and Reactive Black 5 (RB5), produced by Boruta Color Company (Poland), were chosen as the model contaminants for the photocatalytic

decolourisation tests for the produced materials. RR198 and RB5 are water soluble azodyes. Their molecular formulae are presented in Fig. 1. Both dyes exhibit absorption maxima in the spectral range of visible light (RR198-518 nm and RB5-597 nm). Moreover, the light resistances of RR198 and RB5 are 4–5 (ISO Blue Wool Scale). This parameter was estimated by the Boruta Color company, and it is defined according to an eight-unit scale, and corresponds to the amount of dye present in a final product.

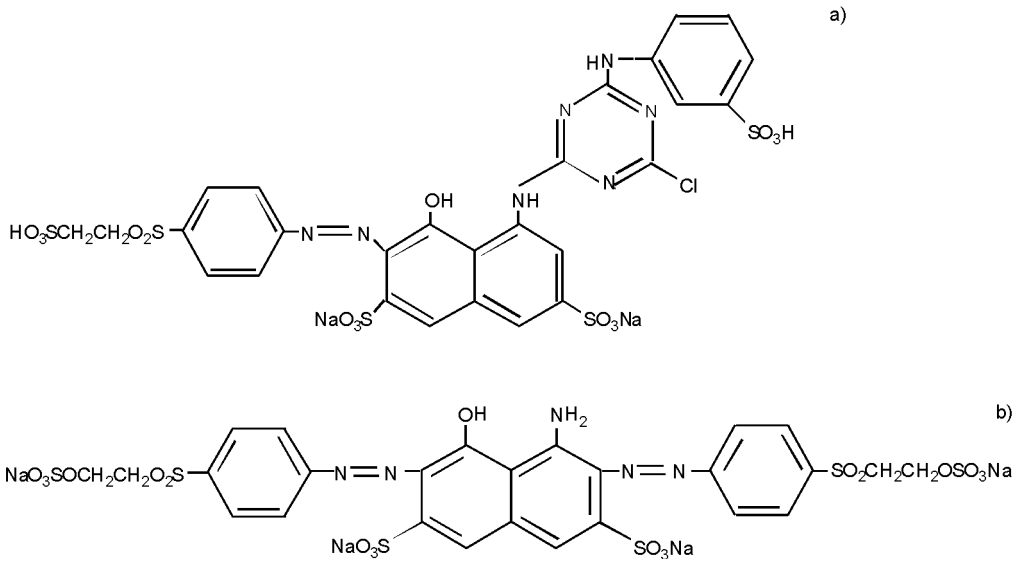

Fig. 1. The molecular formulas of RR198 (a) and RB5 (b)

Preparation of TiO_2 derived nanomaterials. As the first step in the preparation of the nanostructured materials, TiO_2-P25 (2 g) was added to 10 M NaOH aqueous solution (50 cm^3). Afterwards, the as-obtained mixture was kept at 210 °C in a 70 cm^3 autoclave. The annealing time was fixed at 24 h, throughout which the required temperature was maintained. Subsequently, the product of the hydrothermal reaction was washed with distilled water until the pH of the supernatant reached the value of 7. Next, one batch of the obtained powder was collected and dried at 70 °C for 24 h. The sample prepared in the manner described above shall henceforth be referred to, and was labelled as S1. The remaining powder was treated with 0.1 M HCl aqueous solution and was dispersed in an ultrasound bath. Afterwards, this batch was treated repeatedly with distilled water until pH of the supernatant was about 7. Finally, it was dried at 70 °C for 24 h. That sample shall henceforth be referred to, and was labelled as S2.

Experimental procedures and techniques. The morphology of the prepared samples was observed via scanning electron microscopy (SEM, DSM 962, Zeiss, Germany). The crystalline structures of the samples were characterized by X-ray diffrac-

tion (XRD) analysis (X'Pert PRO Philips diffractometer) using a CoK_α radiation. The optical properties of the materials were investigated by means of the diffuse reflectance (DR) UV-Vis technique, using a Jasco (Japan) spectrometer. Additionally, the vibronic properties of the photocatalysts were examined based on their FTIR response. The measurements were performed using a Jasco FTIR 430 (Japan) spectrometer equipped with a diffuse reflectance accessory (Harrick, USA). Resonance Raman analysis was performed using a resonance Renishaw Raman inVia microscope with the laser radiation of the wavelength of 785 nm. And finally, the BET surface areas and mean pore diameters of the catalysts were measured by nitrogen gas adsorption using a Micrometrics ASAP 2010 apparatus.

Determination of photocatalytic activity. The photocatalytic activity of the prepared nanostructure materials was examined by observing the decolourization of the organic dyes when they undergo photocatalytic reaction. The photocatalytic reactions were carried out in an open glass reactor containing 20 cm^3 of a model solution of RR198 or RB5 (initial concentration: 30 mg/dm^3) and 10 mg of the produced materials. At first, the solution was mixed in an ultrasonic bath for half an hour. The solution was subsequently irradiated for 2 h using an 60 W lamp. Next, it was filtered through a 0.45 μm membrane filter. The changes in the concentrations of the dyes were measured using a UV-vis spectrophotometer (Jasco V-530, Japan) at fixed wavelengths of 518 nm (RR198) and 597 nm (RB5).

3. Results and discussion

3.1. Characteristics of the produced materials

Figure 2 shows the SEM images, at two different levels of magnification, of the raw material (pristine TiO_2-P25, images a), b)), and the S1 and S2 samples (images c)–f)). The pristine TiO_2-P25 sample consists of granular crystals with an average diameter of about 25 nm. As is clearly observed, the morphologies of the S1 and S2 samples are clearly different from that of the TiO_2-P25 sample. The S1 sample is composed of rod-like structures. The S2 sample exhibits a similar morphology. It is clearly observed that the mean diameter of S2 nanoparticles is smaller than that of S1 nanoparticles. The rod length distributions of the samples are shown as histograms in Fig. 3: histogram a corresponds to the S1 sample, and histogram b corresponds to the S2 sample. It can be seen that the length of the rods ranges from 1.2 μm to 5.3 μm and from 1.7 μm to 3.2 μm for S1 and S2, respectively. This suggests that acid treatment of S1 leads to an overall reduction in the rod lengths.

The morphology of S2 was studied in greater detail using TEM (data not shown here). One can observe that the S2 sample consists of nanorod particles having an average diameter of 35 nm (ranging from 20 nm to 50 nm). Additionally, the produced nanorods are basically layer-structured, with the layer spacing of 0.96 nm. This value

is higher than those obtained by Meg (0.67 nm) [22], Pavasupree and Yu (0.80 nm) [20, 2] or Tahir (0.32 nm) [24].

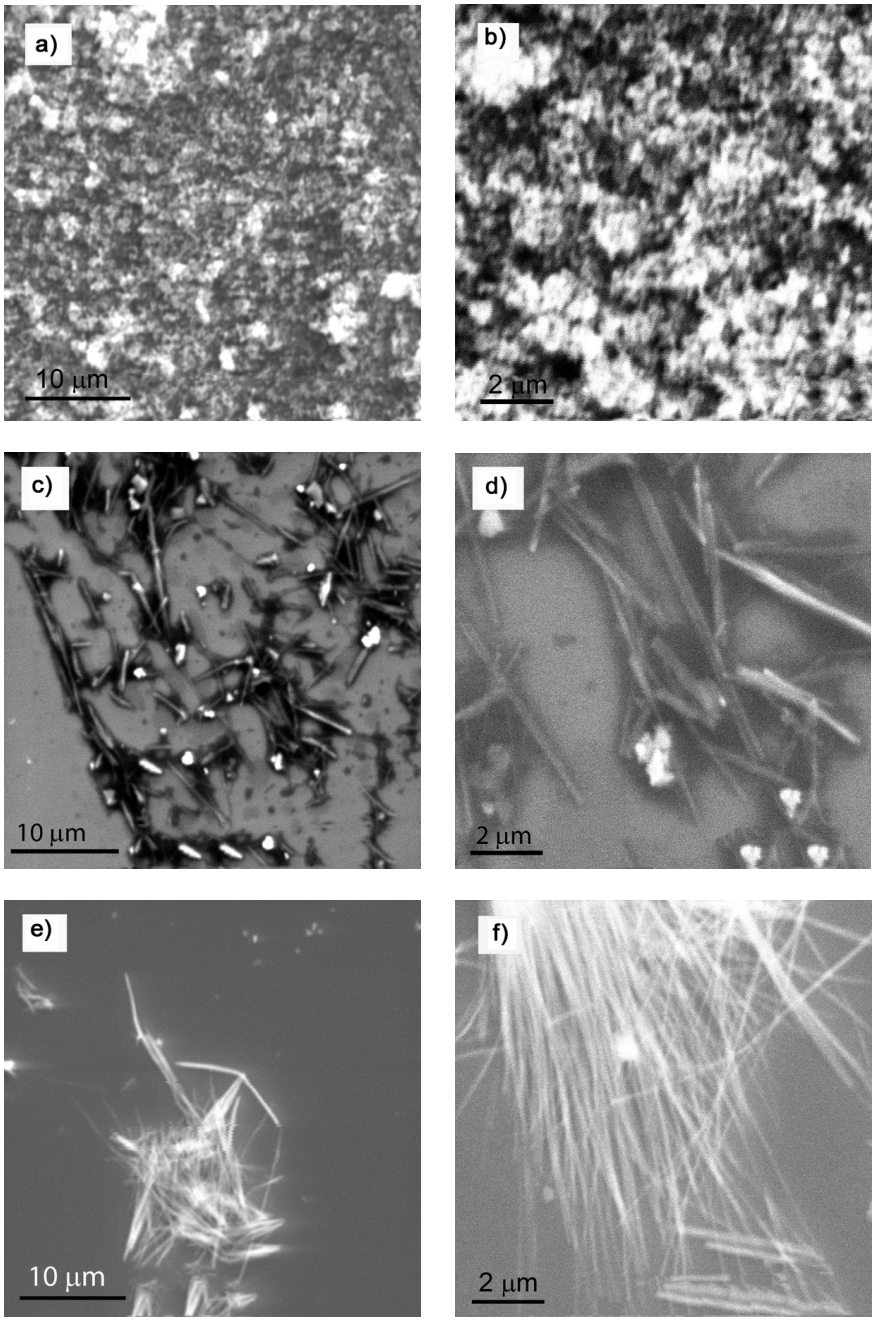

Fig. 2. SEM images of: pristine TiO_2-P25 (a, b), S1 (c, d) and S2 (e, f)

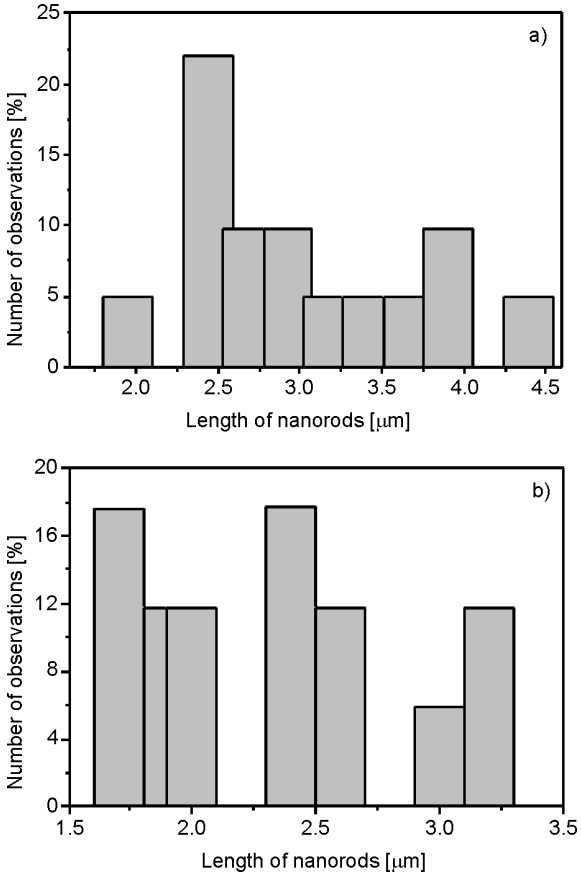

Fig. 3. Distribution of nanorods' lengths: a) S1 and b) S2

The XRD pattern of the pristine TiO_2-P25 sample is presented in Fig. 4a. TiO_2-P25 is a mixture of two different forms of titanium dioxide, such as anatase (marked by the symbol ●, JCPDS card No. 21-1272) and rutile (marked by the symbol ■, JCPDS card No. 34-180). For comparison, Fig. 4b presents the XRD patterns of the samples produced after the hydrothermal reaction and after acid treatment (patterns: 1 – S1, 2 – S2). Detailed phase analysis reveals that S1 is composed of sodium tetra-titanate ($Na_2Ti_4O_9$ marked in Fig. 4b by the symbol ▲, JCPDS card No. 33-1294). One can also observe that S2 (pattern b) is a mixture of sodium titanate (Na_2TiO_3 marked by the symbol ♦, JCPDS card No. 11-0291) and hydrogen pentatitanate ($H_2Ti_5O_{11}\cdot H_2O$ – marked by the symbol ∗, JCPDS card No. 00-044-0131). It is known that K^+ or Na^+ ions in tetratitanates (such as $K_2Ti_4O_9$ or $Na_2Ti_4O_9$) can be exchanged by H^+ ions in HCl aqueous solutions [2]. Therefore, the resulting sample contains hydrogen tetra-titanate $H_2Ti_4O_9$. Here, the interesting point is that during the acid treatment of S1, only partial substitution of sodium by hydrogen atoms, forming $H_2Ti_5O_{11}\cdot H_2O$ occurred. The formation of the additional form of sodium titanate (Na_2TiO_3) is detected.

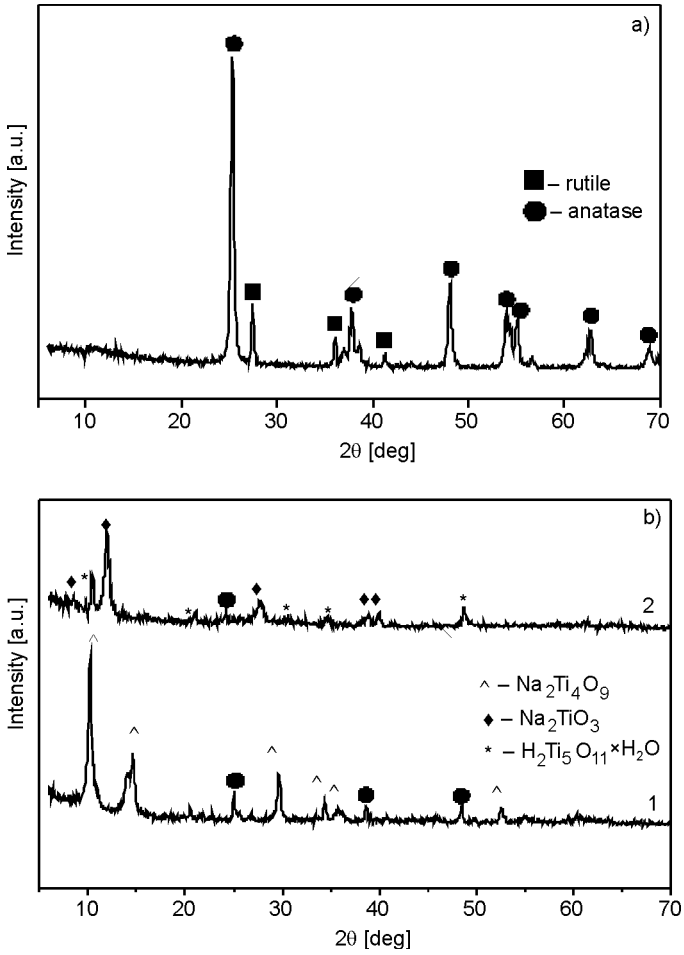

Fig. 4. Diffractograms of the materials: a) pristine TiO_2-P25, b) S1 and S2

The question of what product materials result when NaOH undergoes hydrothermal reaction with different titanium dioxide precursors is the subject of intensive discussions. In many papers, authors argued that TiO_2-derived nanotubes and nanorods are composed of sodium trititanate ($Na_2Ti_3O_7$) and hydrogen trititanate ($H_2Ti_3O_7$) [21, 25, 26]. It is worth pointing out that the nanorod structures of sodium tetratitanate ($Na_2Ti_4O_9$) and hydrogen pentatitanate ($H_2Ti_5O_{11}$), as the main products of hydrothermal reaction of titanium dioxide in NaOH solution have not been described much in the state-of-the-art literature. Furthermore, the presence of anatase phase of TiO_2 can be observed in the diffraction peaks of both the S1 and the S2 samples. It indicates that a small amount of an anatase-type of TiO_2 still remains in the product materials.

Figure 5 shows the FTIR spectra of the pristine TiO_2-P25 sample (spectrum a) and the samples produced after hydrothermal reaction and acid treatment (spectra: b-S1, c-S2).

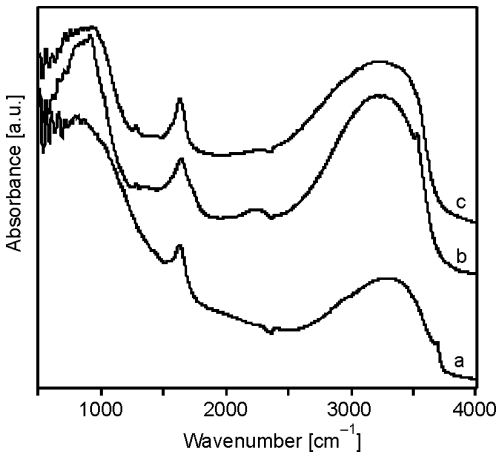

Fig. 5. The FTIR/DRS spectra of: a) pristine TiO_2-P25, b) S1 and c) S2

Absorption bands at about 1000 cm^{-1}, 1640 cm^{-1}, and a very broad band in the 3600–2600 cm^{-1} range were detected in the FTIR spectrum of pristine TiO_2-P25. The band at 1000 cm^{-1} corresponds to the stretching and bending vibrations of Ti–O–Ti bonds [27]. The vibration modes at 1640 cm^{-1} and in the 3600–2600 cm^{-1} range are assigned to the binding vibration of H–O–H and the O–H stretching vibration of the physically adsorbed water [27, 28]. Additionally, here one can notice that the intensities of the bands at 1640 cm^{-1} and 3600–2600 cm^{-1} in the FTIR spectra of S1 and S2 are enhanced with respect to the pristine TiO_2-P25. This indicates that a large amount of adsorbed water remains on the sample surfaces. Moreover, in the case of those two samples, a new absorption band at 1280 cm^{-1} was observed. It is also of note that, for the S1 sample, a new broad band was detected in the 2040–2380 cm^{-1} range.

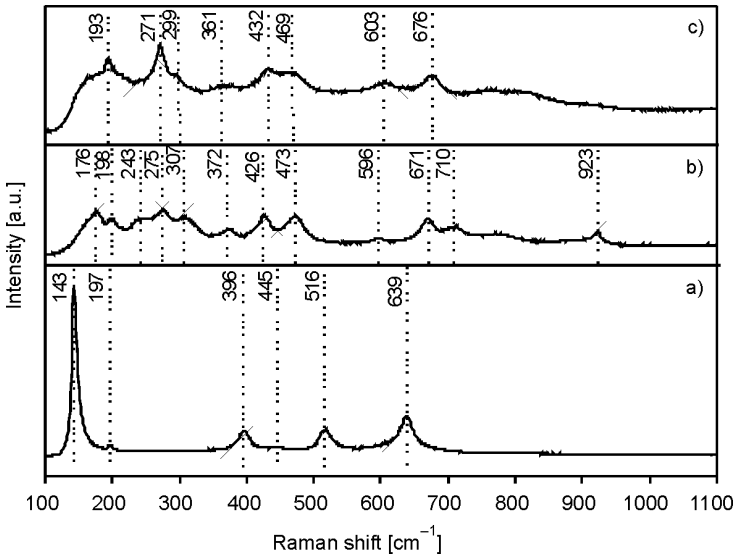

Fig. 6. Raman spectra of: a) pristine TiO_2-P25, b) S1 and c) S2

Figure 6 shows the resonance Raman spectra of the pristine TiO_2-P25 (spectrum a) and produced samples (spectra: S1 – b, S2 – c). It is clearly seen that the spectrum of the TiO_2-P25 shows six peaks at 143, 197, 396, 445 (of very small intensity), and at 516 and 639 cm^{-1}. According to the reference [29, 30], anatase phase of TiO_2 has six Raman active modes ($A_{1g} + 2B_{1g} + 3E_g$) at 147, 198, 398, 515, 640 and 796 cm^{-1}, while rutile has four active modes ($A_{1g} + B_{1g} + B_{2g} + E_g$) situated at 144, 448, 612 and 827 cm^{-1}, respectively. TiO_2-P25, as a mixture of anatase (80%) and rutile (20%), has five Raman peaks (at 143, 197, 396, 516 and 639 cm^{-1}) corresponding to anatase, but just one peak, at 445 cm^{-1}, corresponding to rutile [30].

Additionally, in Figure 6 it is clearly observed that the Raman spectra of S1 and S2 are different from the spectrum of pristine TiO_2-P25. Raman peaks observed for the S1 and S2 nanorods are quite similar to those that have been described before [12, 31]. Moreover, S1 and S2 samples exhibit relatively weak Raman modes in comparison with TiO_2-P25. This observation can be explained by poor crystallinity of the obtained nanorods. In the case of the S1 sample, bands at approximately 176, 198, 243, 275, 307, 372, 426, 473, 596, 671, 710 and 923 cm^{-1} are observed. The Raman modes, at about 176, 198 cm^{-1} and those in the 224–339 cm^{-1} range (namely at 243, 275, and 307 cm^{-1}) are assigned to the stretching modes of Ti–O–Na [12]. The split peaks in the 396–504 cm^{-1} region and the peak at 596 cm^{-1} correspond to the bending and stretching vibration of Ti–O bonds. Moreover, the peak at about 923 cm^{-1} is also attributed to the stretching modes of Ti–O [12, 29, 32]. Additionally, the expected band at 671 cm^{-1} is due to the Ti–O–Ti stretching vibration [23]. In the case of the S2 sample, all the above mentioned bands (except the peaks at about 710 and 923 cm^{-1}) are detected. Additionally, we can state that the Raman peaks having maxima at about 372 cm^{-1} (S1) and 361 cm^{-1} (S2) are probably due to TiO_2 (anatase).

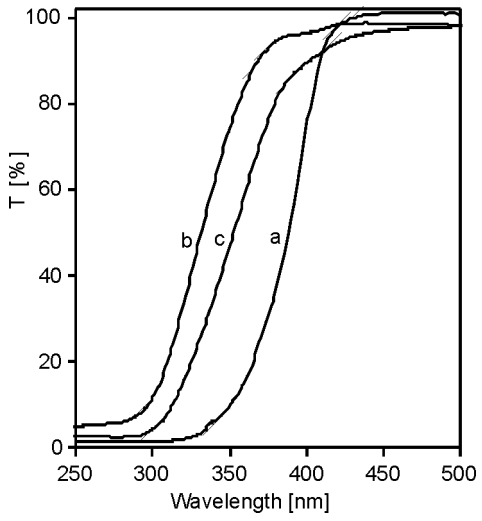

Fig. 7. The DR-UV-vis transmission spectra of: a) pristine TiO_2-P25, b) S1 and c) S2

The DR-UV-vis spectrum of the pristine TiO_2-P25 (spectrum a), as well as the spectra of the S1 and S2 samples (spectra b and c) are presented in Fig. 7. The absorption edges of S1 and S2 shift towards shorter wavelengths in comparison with the pristine TiO_2-P25. The band gap energies of all investigated samples were determined using the DR-UV-vis method and were calculated from the equation:

$$\alpha h\nu = A(h\nu - EG)^r \tag{1}$$

where α is the absorption coefficient, $h\nu$ is the photon energy, EG is the optical band gap, A is a constant which does not depend on the photon energy and r is a parameter equal to 1/2, 3/2, 2 or 3, depending on the type of transition (1/2 for allowed direct, 2 for allowed indirect, 3 for forbidden direct and 3/2 for forbidden indirect optical transitions) [33, 34]. We can state that the band gap energies of the S1 and S2 samples are greater than that for pristine TiO_2-P25. The calculated EG are 3.049, 3.637 and 3.420 eV for TiO_2-P25, S1 and S2, respectively.

Table 1. The band gap values and nitrogen adsorption data for the samples under study

Sample	EG [eV]	BET surface area [m^2/g]	Mean pore diameter [nm]
TiO_2-P25	3.049	52	6.9
S1	3.637	15.6	7.9
S2	3.420	30.3	7.2

Additional characteristic features of the produced nanostructures and the starting material (such as BET surface area, mean pore diameters and band gap energies) are listed in Table 1. According to the manufacturer's data, TiO_2-P25 has the specific surface area of 52 m^2/g and the mean pore diameter of 6.9 nm. The specific surface areas of S1 and S2 samples are lower than that of the pristine TiO_2-P25 sample. For example, the BET surface areas of the S1 and S2 samples are about 3 and 2 times lower, respectively, than that of the TiO_2-P25 sample.

3.2. Photocatalytic reactions

The photocatalytic activities of the produced materials were studied by observing the reaction, specifically the photocatalytic decolourisation, of two organic dyes (Reactive Red 198 – RR198 and Reactive Black 5 – RB5) as model contaminants. At the first stage, the control reaction without catalysts and using RR198 and RB5 solutions (having the concentration of 30 mg/dm^3) was investigated. A small degree of decolourization was observed in both the dyes (RR198 – 5.64%, RB5 – 3.12%) after 2 h of UV irradiation.

Further experiments were conducted using the same organic dyes but contents of all studied materials did not change (10 mg of TiO_2-P25, S1 and S2 on 20 cm^3 of dye solution). Figure 8 shows the decolourization profiles of RR198 and RB5 dyes, in the presence or absence of the considered catalysts, and after being subjected to UV-light irradiation for 2 h. The both organic dyes undergo total decolourization after 1 h of UV illumination, but only for the TiO_2-P25 catalyst. After 2 h of irradiation, the degrees of decolourization of the RR198 and RB5 dyes were 25.7% and 54.9% for the S1 catalyst, and 34.5% and 61.4% in the case of the S2 catalyst. Furthermore, Figure 8 also shows that the sample obtained after acid treatment (S2) exhibits higher catalytic activity than the one obtained directly after hydrothermal reaction (S1).

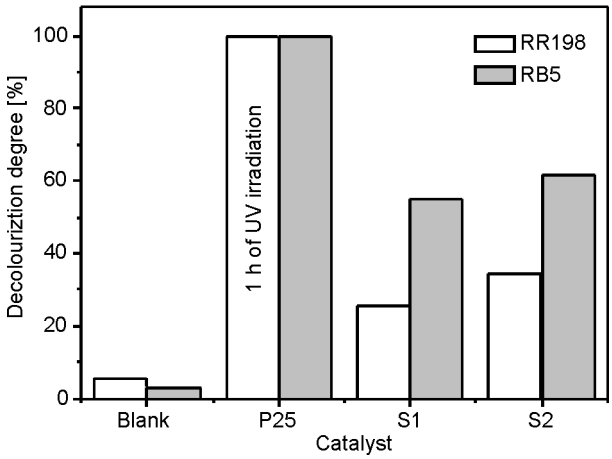

Fig. 8. Photocatalytic decomposition of RR198 and RB5 in the presence of the pristine TiO_2-P25 and S1 and S2 samples

As is well known, the catalytic activity of a catalyst material is directly proportional to its BET surface area. Pristine TiO_2-P25 exhibits the highest BET surface area (52 m^2/g) and the highest photocatalytic activity in the dye decolourization reaction. Moreover, one can observe that the BET surface areas of the produced samples decreased considerably after the hydrothermal reaction (S1, 15.6 m^2/g) and subsequently increased after acid treatment (S2, 30.3 m^2/g). As is clearly observed from the data, there is a direct correlation between the BET surface area and the degree of dye decolourization: the higher the BET surface area, the higher the degree of decolourization of the RR198 and RB5 dyes (TiO_2-P25 > S2 > S1). Additionally, it is worth pointing out that RR198 and RB5 dyes are not adsorbed on the S1 and S2 surfaces. It is known that the adsorption of the reagents on the surface of the photocatalyst is a very important consideration in the photocatalytic process. This might be a possible reason why the nanostructures described here exhibit less photocatalytic activity, compared with the TiO_2-P25 sample, in the dye decolourisation reaction. Detailed studies to verify the proposed explanation are currently in progress.

4. Conclusions

The syntheses and detailed characterization of TiO_2-derived nanorods using commercial TiO_2-P25 as a precursor have been described. The obtained nanorods having an average length of 5.9 μm (after the hydrothermal reaction) and 4.05 μm (after the hydrothermal reaction and acid treatment) revealed to be a composition of different layers of titanates ($Na_2Ti_4O_9$, Na_2TiO_3, $H_2Ti_5O_{11}\cdot H_2O$). Additionally, it was proved that the fabricated nanorods are less active in the photocatalytic reaction of decolourisation of organic dyes than pristine TiO_2-P25. Furthermore, we have proved that the nanorods synthesized from pristine TiO_2-P25 exhibit higher photocatalytic activity than the nanorods synthesized either from hydrothermally treated TiO_2-P25 (referred to as material S1 in this paper) or from hydrothermal-and-acid-treated TiO_2-P25 (referred to as material S2 in this paper).

Acknowledgements

This work was sponsored by the Polish State Committee for Scientific Research, under grant N523 025 32/0983 (B. Z.).

References

[1] KASUGA T., HIRAMATSU M., HOSON A., SEKINO T., NIIHARA K., Langmuir, 14 (1998), 3160.
[2] YU H., YU J., CHENG B., ZHOU M., J. Solid State Chem., 179 (2006), 349.
[3] WU D., LIU J., ZHAO X., LI A., CHEN Y., MING N., Chem. Mater., 18 (2006), 547.
[4] LIU L., ZHANG Y., Sensor Actuat A., 116 (2004), 394.
[5] CHEN C.-C., YEH C.-C., LIANG C.-H., LEE C.-C., CHEN C.-H., YU M.-Y., LIU, L.C. CHEN H.-L., J. Phys. Chem. Solids, 62 (2001), 1577.
[6] BOROWIAK-PALEN E., PICHLER T., GRAFF A., KALENCZUK R.J., KNUPFER M., FINK J., Carbon, 42 (2004), 1123.
[7] LI Y., WANG J., DENG Z., WU Y., SUN X., YU D., YANG P., J. Am. Chem. Soc., 123 (2001), 9904.
[8] NATH M., RAO C.N.R., J. Am. Chem. Soc., 123 (2001), 4841.
[9] NIAN J-N., TENG H., J. Phys. Chem. B., 110 (2006), 4193.
[10] WU Q., HU Z., WANG X., J. Am. Chem. Soc., 125 (2003), 2024.
[11] ARNOLD M.S., AVOURIS P., PAN Z., J. Phys. Chem. B., 107 (2003), 659.
[12] KOLEN'KO Y.V., KOVNIR K.A., GAVRILOV A.I., GARSHEV A.V., FRANTTI J., LEBEDEV O.I., CHURAGULOV B.R., TENDELOO G. V., YOSHIMURA M., J. Phys. Chem. B., 110 (2006), 4030.
[13] XU C., ZHAN Y., HONG K., WANG G., Solid State Commun., 126 (2003), 545.
[14] ZHU Y., LI H., KOLTYPIN Y., HACOHEN Y.R., GEDANKEN A., Chem. Commun., 24 (2001), 2616.
[14] KASUGA T., HIRAMATSU M., HOSON A., SEKINO T., NIIHARA K., Adv. Mater., 11 (1999), 1307.
[15] JR E.M., ABREU M.A.S., PRAVIA O.R.C., MARINKOVIC B.A., JARDIM P., RIZZO F.C, ARAUJO A.S., Solid State Sci., 8 (2006), 888.
[16] CHEN Q., DU G.H., ZHANG S., PENG L.M., Acta Crystallogr. B., 58 (2002), 587.
[17] YANG D.B., CHAN Y.F., ZHANG X.Y., ZHANG W.F., YANG Z.Y., WANG N., Appl. Phys. Lett., 82 (2003), 281.
[18] SUN X., LI Y., Chem.-Eur. J., 9 (2003), 2229.
[19] PAVASUPREE S., SUZUKI Y., YOSHIKAWA S., KAWAHATA R., J. Solid State Chem., 178 (2005), 3110.
[20] YOSHIDA R., SUZUKI Y., YOSHIKAWA S., Mater. Chem. Phys., 91 (2005), 409.

[21] MA Y., LIN Y., XIAO X., ZHOU X., LI X., Mater. Res. Bull., 41 (2006), 237.
[22] MENG X., WANG D., LIU J., ZHANG S., Mater. Res. Bull., 39 (2004), 2163.
[23] TAHIR M.N., THEATO P., OBERLE P., MELNYK G., FAISS S., KOLB U., JANSHOFF A., STEPPUTAT M., TREMEL W., Langmuir, 22 (2006), 5209.
[24] KASUGA T., Thin Solid Films, 496 (2006), 141.
[25] WEI M., KONISHI Y., ZHOU H., SUGIHARA H., ARAKAWA H., Solid. State Commun., 133 (2005), 493.
[26] YU L., ZHANG X., Mater. Chem. Phys., 87 (2004), 168.
[27] ŠTENGL V., BAKARDJIEVA S., ŠUBRT J., VEČERNIKOVA E., SZATMARY L., KLEMENTOVA M., BALEK V., Appl. Catal. B., 63 (2006), 20.
[28] MA R., FUKUDA K., SASAKI T., OSADA M., BANDO T., J. Phys. Chem. B., 109 (2005), 6210.
[29] QIAN L., DU Z-L., YANG S-Y., JIN Z-S., J. Mol. Struct., 749 (2005), 103.
[30] PAPP S., KOROSI L., MEYNEN V., COOL P., VANSANT E.F., DEKANY I., J. Solid State Chem., 178 (2005), 1614.
[31] MENZEL R., PEIRÓ A.M., DURRANT J.R., SHAFFER M.S.P., Chem. Mater., 18 (2006), 6059.
[32] LARRUBIA M.A., RAMIS G., BUSCA G., Appl. Catal. B., 27 (2000), L145.
[33] HASAN M.M., HASEEB A.S.M.A., SAIDUR R., MASJUKI H.H., PWASET, 30 (2008), 221.
[34] BERNARDI M.I.B., LEE E.J.H., LISBOA-FILHO P.N., LEITE E.R., LONGO E., VARELA J.A., Mat. Res., 4 (2001) 223.

Received 20 February 2008
Revised 21 September 2009